ELSEVIER

PII: S0032-3861(97)00378-9

Polymer Vol. 39 No. 10, pp. 1921–1927, 1998

0032-3861/98/$19.00+0.00

Cocrystallisation in blends of poly(vinylidene fluoride) samples: 4. Kinetics study

Jhunu Datta and Arun K. Nandi*
Polymer Science Unit, Indian Association for the Cultivation of Science, Jadavpur, Calcutta-700 032, India
(Received 30 January 1997; revised 18 March 1997)

The overall crystallisation rates of poly(vinylidene fluoride) (PVF_2) samples [KF PVF_2; head to head defect = 3.5 mol%, KY PVF_2 head to head defect = 5.3 mol%] and their cocrystals are measured. At the same undercooling (ΔT) the crystallisation rate of cocrystals is faster than that of the pure component with identical head to head defect concentration. The isothermal temperature range and the Avrami exponent vary linearly with composition. Analysis of the crystallisation rate using Lauritzen–Hoffman growth rate theory indicates regime I–II transition of KF PVF_2 sample and regime II–III transition for KY PVF_2 and their cocrystals. The product of surface free energies ($\sigma\sigma_e$) is lower for the cocrystal than that of the pure component. Assuming the fold surface energy (σ_e) as invariant for the above two PVF_2 samples, the lateral surface energy (σ) values are calculated and have been interpreted according to a recent theory of Hoffman *et al.* (*Macromolecules*, 1992, **25**, 2221) The results indicate a small extension of the PVF_2 chains in the melt of the blend. The entropy of cocrystallisation has been calculated from the above theory and has been found to be ~0.6 cal deg^{-1} mol^{-1}. A model for explaining the higher crystallisation rate of the cocrystal compared with that of the pure components at the same ΔT has been presented.

(Keywords: PVF_2; crystallisation regime; chain characteristic ratio)

INTRODUCTION

Poly(vinylidene fluoride) (PVF_2) is a technologically important polymer because of its piezoelectric property[1]. The polymer is not completely isoregic but has different amounts of head to head defect (H–H) structure in the chain[2].

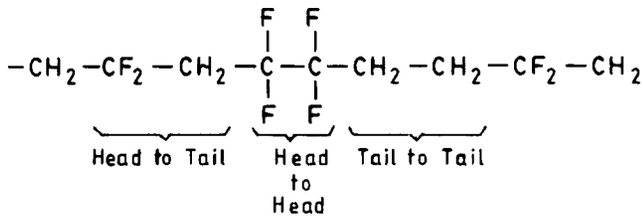

These H–H defects enter into the crystalline lamella, affecting its physical properties[3,4]. In our earlier papers we have reported a detailed study of the factors affecting the cocrystallisation[5,6]. In this paper we want to shed light on the mechanism of cocrystallisation from a study on the crystallisation rate.

Some reports on the crystallisation rate of cocrystals of polyethylene are found in the literature[7–10]. Ree *et al.*[7] observed an intermediate crystallisation rate for the blend compared with that of the components at the same crystallisation temperature (T_c). Iragorri *et al.*[8] also observed similar intermediate growth rate of the cocrystals, the growth rate increases with increasing the linear component in the blend of linear and branched polyethylene at a given T_c. Tashiro *et al.*[9,10] measured the crystallisation rate of polyethylene blends using time-resolved *FT*i.r. and time resolved SAXS instruments, but they observed higher crystallisation rates of the cocrystals than those of the components at the same undercooling. However, there is no report on the crystallisation rate of cocrystals other than polyethylene and here the crystallisation mechanism of PVF_2 and of their cocrystals with different H–H defect content components has been delineated from the crystallisation rate measurement.

In this paper, comparison of the crystallisation rates, isothermal temperature range (T_R) for crystallisation within the same time scale, Avrami exponents (n), etc. have been made between the cocrystals and the components. The crystallisation rates have been analysed using the Lauritzen–Hoffman (L–H) theory[11,12] of polymer crystallisation. From the surface energy values (obtained from the above analysis) and using a recent theory of Hoffman *et al.*[13] this paper attempts to get an idea on the chain configuration at the melt of the blend and also attempts to calculate the entropy of cocrystallisation of the cocrystals.

EXPERIMENTAL

The characteristics of the PVF_2 samples and the cocrystals used for the kinetics study are presented in *Table 1*[5,6]. The commercial samples were recrystallised from its dilute solution in acetophenone and after repeated washing with methanol the samples were dried in vacuum at 60°C for 3 days. The cocrystals were prepared using a procedure mentioned earlier[5]. The crystallisation kinetics have been measured using a Perkin–Elmer Differential Scanning Calorimeter (DSC-7) equipped with a 3700 data station. The samples (~5 mg) were placed in aluminium pans and melted in d.s.c. at 227°C for 10 min to destroy all homogeneous nuclei[14]. Then they were quenched to the isothermal crystallisation temperature (T_c) and crystallised

* To whom correspondence should be addressed

Table 1 Characteristics of PVF_2 samples and their cocrystals used in this work

System	Composition W_x	$\bar{M}_w \times 10^{-5}$	H–H defect (mol%)	T_m^0 (°C)
KF-1000(KF)/KY-201 (KY)	0.0	4.28	3.50	212
	0.27			202
	0.49			197.4
	0.74			186
	1.00	7.36	5.31	189

W_x, weight fraction of KY PVF_2

for a predetermined time period. The samples were scanned from that temperature at the rate of 10°C min^{-1} without cooling. The enthalpy of fusion was determined from the area of the endothermic peak(s) by comparing with the heat of fusion of a standard indium sample. Values of the level of crystallinity $(1 - \lambda)_{\Delta H}$, were determined taking the enthalpy of fusion per repeating unit $(\Delta H_u^0) = 104.5\ J\ g^{-1}$[15]. The uncertainty in the measurement of crystallinity is within ± 2%. The experiment was repeated for other crystallisation conditions. The representative melting endotherms obtained for different times of crystallisation have been shown in *Figure 1a*. The Greek symbols (α, γ and γ′) in the figure indicate the melting of α, γ and γ′ polymorphs of PVF_2 produced during the crystallisation[16].

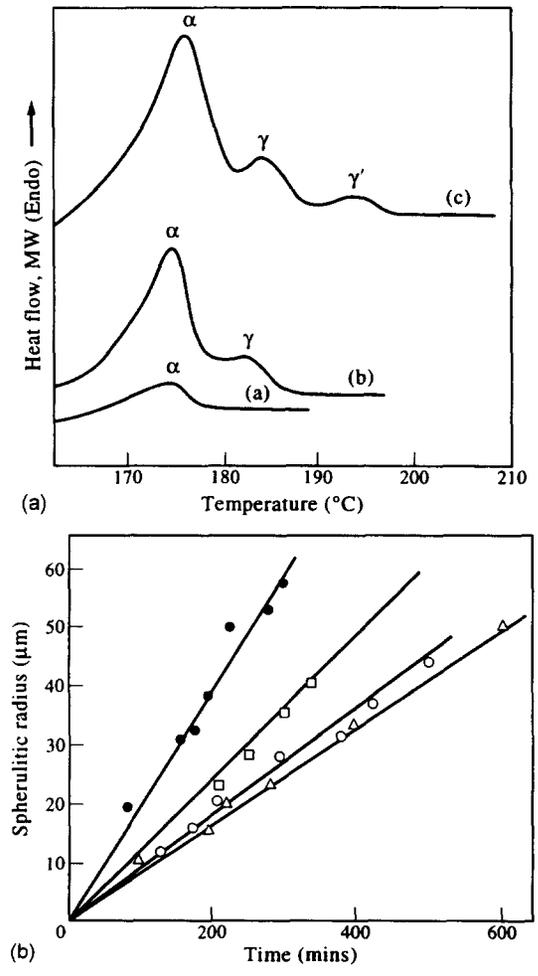

Figure 1 (a) Melting endotherms of KF/KY PVF_2 blend ($W_{KY} = 0.49$) showing three different polymorphs (α, γ, and γ′) produced by crystallising at 162°C for (a) 30 min, (b) 120 min and (c) 1000 min. (b) Representative plots for spherulitic radius with time for PVF_2 samples (α phase): ● W_{KY} = 0.0 at 168°C; ○, $W_{KY} = 0.25$ at 166°C; □, $W_{KY} = 0.75$ at 162°C; △, W_{KY} = 1.0 at 156°C

The equilibrium melting points T_m^0 presented in *Table 1* are taken from Ref. [6]. In some cases, we also measured the growth rates of α-spherulites of PVF_2 using Mettler FP-82 hot stage and a Leitz polarising microscope fitted with a semiautomatic camera system. The growth of the α-spherulites is linear with time at all values of T_c for all samples (*Figure 1b*). From the least square slopes of the plots growth rates have been calculated.

RESULTS AND DISCUSSION

Crystallisation isotherms

In *Figure 2a–e* the crystallisation isotherms of KF and KY PVF_2 and their cocrystals produced at the weight fractions of KY PVF_2 (W_{KY}) of 0.27, 0.49 and 0.74 have been presented. Each isotherm, like the crystallisation isotherms of other polymers, exhibits autocatalytic nature and finally there is a retardation in the crystallisation rate corresponding to the tail part of the isotherms[17]. PVF_2 crystallises from the melt in three different polymorphs (α,

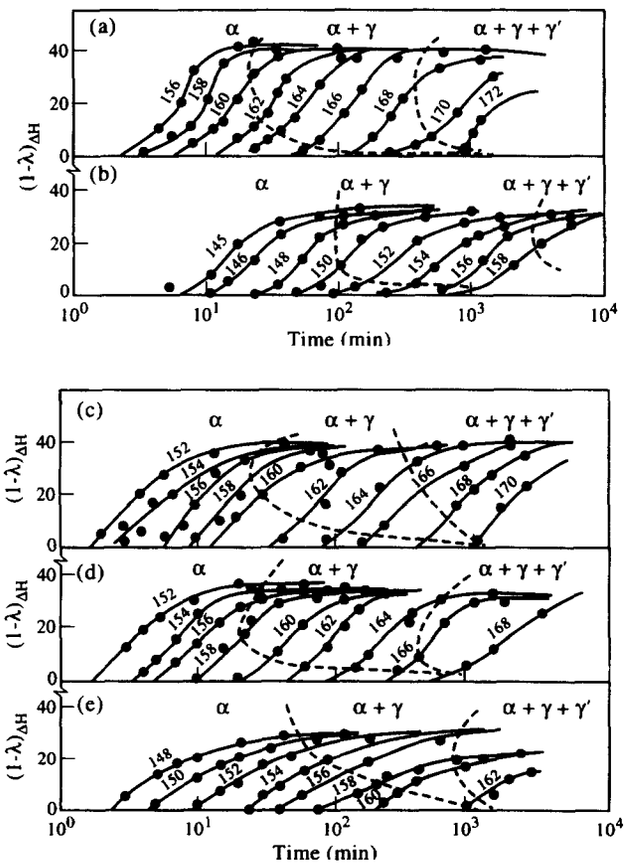

Figure 2 Plots of degree of crystallinity *versus* log time (min) for the KF/KY PVF_2 blends: (a) $W_{KY} = 0$; (b) $W_{KY} = 1$; (c) $W_{KY} = 0.27$; (d) $W_{KY} = 0.49$; (e) $W_{KY} = 0.74$

γ and γ') depending on the temperature and time of crystallisation, γ and γ' phases have been observed only at high T_c for longer time of crystallisation[16]. In the figures, the formation of α, $\alpha+\gamma$ and $\alpha+\gamma+\gamma'$ phases is indicated by dotted lines from the first appearance of the melting peak of the respective phases in the melting endotherms.

In *Figure 3* the effect on the isothermal crystallisation temperature range (T_R) of KF PVF_2 by blending with KY PVF_2 in the same time scale of crystallisation (1–3 decade, min) is presented. It is clear from the figure that with increasing KY PVF_2 in the blend there is an almost linear decrease of T_R. This is because the KY PVF_2 has a higher H–H defect content than that of KF PVF_2 (*Table 1*) and it is difficult to crystallise the higher defect-containing material at the same T_c. So KY PVF_2 crystallises isothermally within the same time scale at lower T_c values than the lower defect content KF PVF_2. Therefore, the above linear decrease of T_R with W_{KY} indicates a perfect cocrystallisation of KF and KY PVF_2 at all the compositions and this has also been observed from the thermodynamic study[6].

In *Figure 4* the overall crystallisation rates ($\tau_{0.1}^{-1}$, where $\tau_{0.1}$ is time required to attain 10% crystallinity) of the cocrystals have been compared for different blend compositions and also for different values of T_c. At each T_c with increase in KY PVF_2 in the blend the crystallisation rate decreases. However, the decrease in crystallisation rate is not exactly linear but they are very well fitted in slightly concave upward curves. This indicates that there is negative deviation from the line joining the rates of the two components. However, to make a meaningful comment on the composition dependence of the overall crystallisation rate it should be plotted on the same undercooling basis for all the compositions. In *Figure 5* the composition dependence of the crystallisation rate at the same undercooling has been presented. From the figure it is clear that it shows some positive deviation from linearity and there is a maximum at $W_{KY}=0.74$. This is also true for the growth rate of the α spherulites. Assuming that T_g of KF PVF_2 and KY PVF_2 is the same, at the same undercooling the crystallisation rate/growth rate should remain invariant with blend composition. The positive deviation from linearity is an exception and the reason for such positive deviation will be discussed later.

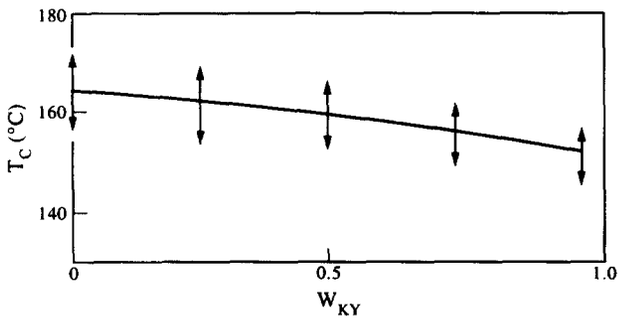

Figure 3 Plot of isothermal crystallisation temperature range (T_R) *versus* blend composition of KF/KY blends

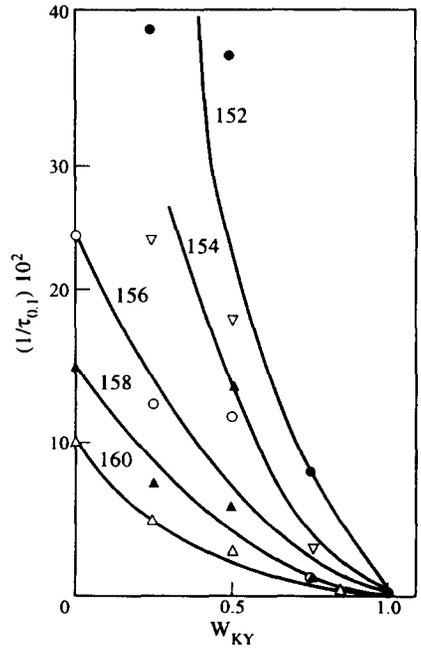

Figure 4 Plots of crystallisation rate ($\tau_{0.1}^{-1}$) *versus* composition of KF/KY PVF_2 blends at indicated T_c values

Avrami analysis

The Avrami equation[18] for the nucleation and growth of a nucleus is given by

$$1-\lambda(t)=1-\exp^{-kt^n} \qquad (1)$$

where $1-\lambda(t)$ is crystallinity at time t, k is the overall rate constant and n denotes the nature of nucleation and growth process. $(1-\lambda)_{\Delta H}$ has been plotted with time (t) on double logarithmic scale for the low level of crystallinity[17] and from the least square slope of the plots Avrami exponents are calculated and are presented in *Table 2*. It is clear from the table that the n values lie between 3 and 2. Thus, according to the theory[17,18] the crystallisation of KF PVF_2 KY PVF_2 and their blends occurs by two dimensional heterogeneous nucleation with linear growth. The Avrami exponent values are close to those of other workers for this polymer[19–21]. In *Figure 6* the plots of Avrami exponents with blend composition has been shown for both at the same T_c and at the same undercooling (ΔT). The plots are linear for both cases.

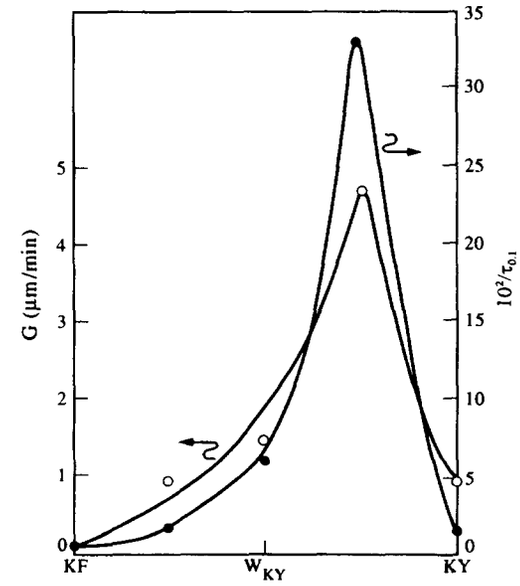

Figure 5 Plots of crystallisation rate *versus* composition of KF/KY PVF_2 at the same undercooling ($\Delta T=40$°C): ●, $\tau_{0.1}^{-1}$; ○, growth rate (G)

Table 2 Values of Avrami exponents (n) for KF/KY PVF_2 systems and their cocrystals at different T_c values

Comp. (W_{KY})	T_c (°C)													
	146	148	150	152	154	156	158	160	162	164	166	168	170	172
0.00	–	–	–	–	–	2.0	2.2	2.0	2.0	2.9	2.5	2.2	2.2	2.4
0.27	–	–	–	2.5	3.5	2.8	2.9	3.7	3.7	2.9	2.9	3.1	–	–
0.49	–	–	–	2.3	2.2	2.7	3.5	2.2	2.2	2.6	2.2	–	–	–
0.74	–	2.6	3.1	2.0	2.0	2.0	2.0	2.3	2.3	–	–	–	–	–
1.00	3.00	3.1	2.6	1.9	2.4	2.0	–	–	–	–	–	–	–	–

Kinetic nucleation theory

Hoffman *et al.*[11,12] propounded the kinetic nucleation theory for the crystallisation of pure polymeric melt from the consideration of the chain folding process, during crystallisation. Since spherulitic growth is linear with time (*Figure 1b*) for all samples (pure and blend) at all T_c values (like a homopolymer), the Lauritzen–Hoffman (L–H) growth rate theory can be applied using the respective T_g and T_m^0 values of the samples[8,9,22]. According to this theory[11,12] the growth rate G is usually expressed as

$$G = G_0 \exp \frac{-U^*}{R(T_c - T_\alpha)} \exp[-K_g(i)/T(\Delta T)] \qquad (2)$$

where G_0 is the pre-exponential factor, U^* is the activation energy of transport, $T_\alpha = (T_g - 30°)$K, T_c is the temperature of crystallisation, $\Delta T = T_m^0 - T_c$ where T_m^0 is the equilibrium melting point of the crystal in the blend and $K_g(i)$ is the nucleation constant of regime (i): $K_g(I) = 2K_g(II) = K_g(III)$ with $K_g(I) = 4b\sigma\sigma_e T_m^0/k\Delta H_f$, where σ and σ_e are the lateral and end surface free energies, respectively. b is the stem length, k is the Boltzmann constant and ΔH_f is the enthalpy of fusion per unit volume.

In this system there is a complicacy in analyzing the overall kinetic data because PVF_2 crystallises into α and γ polymorphs by nucleation from the melt[16]. But it is clear from *Figures 1 and 2* that γ and γ' phases are produced after the α phase. Therefore, the L–H growth rate theory can be applied to the α phase of PVF_2 at the low conversion (~2%) of the melt where γ phase is absent. The inverse of time required to attain 2% crystallinity ($\tau_{0.02}^{-1}$) is considered as the crystallisation rate of α-phase and we have analysed the data according to equation (2). The contribution of the transport term of equation (2) is considered here to be negligible because the isothermal crystallisation temperatures are much higher than the T_g of the systems (T_g, PVF_2 = −39°C[23]) and also the T_R is small (16–18°C). In *Figure 7* plots have been made with ln $1/\tau_{0.02}$ against the temperature function ($T_m^0/T_c\Delta T$) for KF PVF_2, KY PVF_2 and their cocrystals of different compositions. From the figure it is clear that none of the data in each set can be fitted in a single straight line and it is apparent from the figure that KF PVF_2 exhibits I–II regime break while the KY PVF_2 and the cocrystals exhibit regime II–III break*. The present results on the crystallisation regimes are in good agreement with those of other workers[24–26].

The regime transition temperatures of pure PVF_2 samples and those of the cocrystals are presented in *Table 3*. From the table it is clear that as the defect content of KY PVF_2 in the blend increases there is a gradual decrease in regime II–III transition temperature. However, the undercooling (ΔT) at this transition temperature for the different compositions of the blend is almost the same (35 ± 2°C). This supports the kinetic nucleation theory for crystallisation of polymers in different regimes. The $\sigma\sigma_e$ values were calculated from the slopes of each part of the straight lines of *Figure 7* using equation (2). In *Table 4* $\sigma\sigma_e$ values are presented with their uncertainties in measurement. Comparing the $\sigma\sigma_e$ values of any particular regime, it is apparent that the $\sigma\sigma_e$ values show a negative deviation from linearity. This explains the higher crystallisation rate of the cocrystals compared with the components under the same undercooling (cf. *Figure 5*).

The reason for such a negative deviation of $\sigma\sigma_e$ values from linearity is delineated here. The σ_e is related to chain folding (q) by[11]

$$\sigma_e = q/2ab \qquad (3)$$

where ab represents the cross sectional area of the polymer molecules (a is the width of the molecular layer). The σ_e,

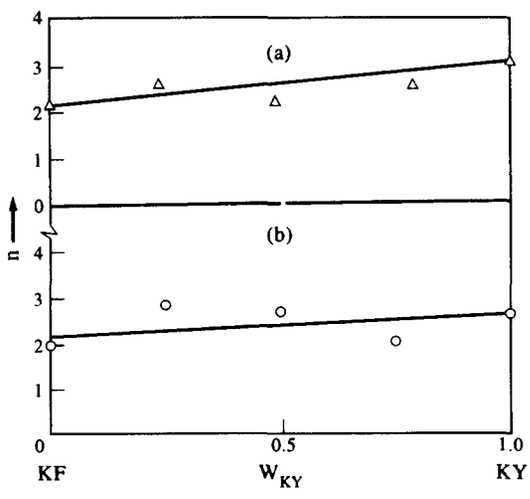

Figure 6 Plot of Avrami exponent n *versus* blend composition, at the same T_c (156°C) (△) and at the same undercooling (40°C) (○)

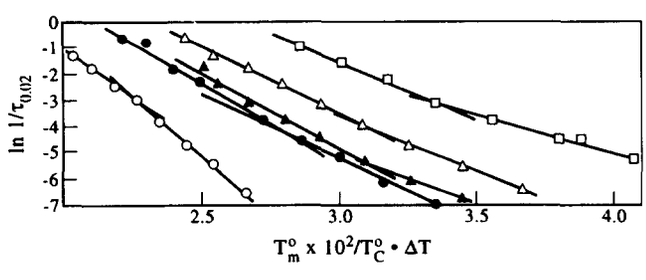

Figure 7 Plot of ln $1/\tau_{0.02}$ *versus* $T_m^0/T_c\Delta T$ for KF/KY PVF_2 blends: ○, $W_{KY} = 0$; ●, $W_{KY} = 0.27$; ▲, $W_{KY} = 0.49$; △, $W_{KY} = 0.74$; $W_{KY} = 1.00$

* Analysis of growth rate data of α-PVF_2 also yields similar regime transition.

Table 3 Regime III–II transition temperatures of PVF_2 (KF and KY) and their cocrystals

Composition (W_{KY})	Trans. pt. T^* (°C)	ΔT ($T_m - T^0$)*
0.00	164	48
0.27	163	39
0.49	162	35
0.74	154	32
1.00	155	34

Table 4 $\sigma\sigma_e$ (erg^2 cm^{-4}) of KF PVF_2, KY PVF_2 and their cocrystals

Composition	$\sigma\sigma_e$		
W_{KY}	Regime I	Regime II	Regime III
0.00	1365 ± 66	2166 ± 39	
0.27		1532 ± 7	909 ± 3
0.49		1176 ± 49	790 ± 9
0.74		904 ± 49	651 ± 30
1.00		1096 ± 49	795 ± 42

therefore, is intramolecular in origin[11], so σ_e may be considered constant for the PVF_2 samples used here. On the other hand, σ can be physically interpreted in two ways[13].

(1) From the chain configuration point of view, σ relates the characteristic ratio (C_α) of the chain of the melt:

$$\sigma = \Delta H_f(a/2)(l_b/l_u)(1/C_\alpha) \quad (4)$$

where l_b is the C–C bond length and l_u is the projected bond length in the chain direction.

(2) From the thermodynamic view point it indicates the loss of entropy in transformation of the coil (I) to the activated state (II) prior to crystallographic attachment

$$\Delta S_{I-II} = -2b\sigma l_u n^* / T_m^0 \quad (5)$$

where l_u is projected bond length in the chain direction and n^* is the number of carbon atoms at the initial fold length (l_g*). From the $\sigma\sigma_e$ values, σ values are calculated taking $\sigma_e = 65$ erg cm^{-1} [21,25].

Chain configuration of the melt

The C_α of the polymer chains in the melt have been calculated using equation (4) and taking $\Delta H_f = 2.01 \times 10^9$ erg cm^{-3} [15], $a = 5.43$ Å[27] and $l_b/l_u = 1.21$ (making the assumption that it is the same as in polyethylene[13]). The values are plotted in *Figure 8* and it is apparent from the figure that for the cocrystals the C_α values are higher than the arithmetic average of the components; the possible cause of this is given below.

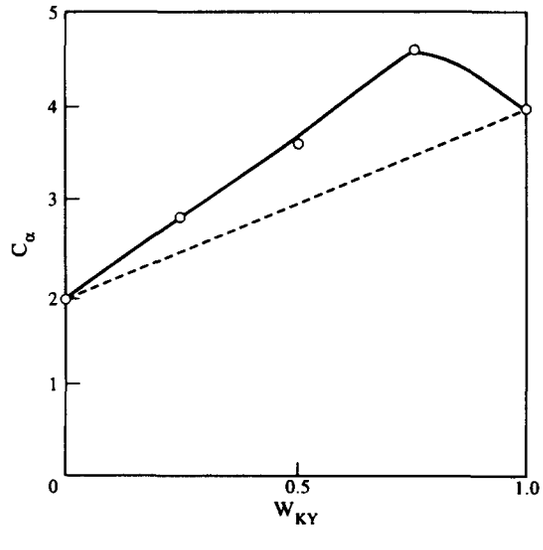

Figure 8 Plot of C_α *versus* blend composition for KF/KY PVF_2 blends

Table 5 Chain extension factor (α), entropy of activation (ΔS_{I-II}) and entropy of cocrystallisation ($\Delta S_{cocrystal}$) of KF/KY PVF_2 blends

Blend	Comp. W_{KY}	α	ΔS_{I-II} (e.u)	ΔS_{cocrys} (e.u)
KF/KY	0.0	1.0	2.00 (± 0.03)	0.00
	0.27	1.10	− 1.45 (± 0.03)	0.40
	0.49	1.13	− 1.12 (± 0.04)	0.60
	0.74	1.16	− 0.88 (± 0.04)	0.66
	1.00	1.00	− 1.43 (± 0.04)	0.00

The C_α value in the pure melt is equal to $\bar{r}_0^{-2}/nl_b^2$ where $\bar{r}_0^{-2}$ is mean square unperturbed end to end distance and n is the number of monomeric units in the chain[28]. In the melts of blends the chains may be extended by a factor α due to the favourable interaction of the components[25,29] and is given by

$$\alpha = \left(\frac{C_\alpha^{cocrystal}}{C_\alpha^{pure}} \right)^{1/2} \quad (6)$$

where $C_\alpha^{cocrystal}$ indicates the characteristic ratio of the cocrystal and C_α^{pure} indicates the C_α value at that blend composition obtained from the line joining those of the components. The chain extension factors calculated from the results are shown in *Table 5*. From these values it can be concluded that there is chain extension* at the melt of the blend compared with its pure components†.

Entropy of cocrystallisation

From equation (5), $\Delta S_{I \rightarrow II}$ for each case has been calculated taking $b = 4.45 \times 10^{-8}$ cm, $l_u = (1.54/1.21) \times 10^{-8}$ cm and $n^* = 2.67 \times 10^{22}$ ml^{-1} (calculated taking $a = 5.43$ Å, $b = 4.45$ Å[27] and $l_b = 1.54$ Å). The $\Delta S_{I \rightarrow II}$ values have been presented in *Table 5*. The entropy of activation is plotted against composition (*Figure 9*) and it is clear from the figure that the entropy of activation is higher for the cocrystals than the line joining that of the components (accounting the − ve sign). This can be deduced from a pictorial presentation (*Figure 10*) of the crystallisation process of pure component and of the blend. In the melt of the blend the polymer chains are already extended (ordered) compared with the pure component, so the entropy loss will be smaller for the blend to form the localised structure (activated state). This lower entropy loss to form the activated complex contribute (through the free energy of activation) to the higher crystallisation rate of cocrystal than that of the pure component.

* The small value of α probably arises due to small favourable interaction of KF and KY PVF_2. The T_m^0-composition plot for this system is slightly concave upward[6], indicating small favourable interaction present in the system[30]. However, these α-values are much smaller than in systems where blending occurs due to large specific interaction[25,29].

† By the pure component it is meant that the H–H defect is the same as in the cocrystal but the structural polydispersity (with respect to H–H defect) is less and equal to the arithmetic average of KF PVF_2 and KY PVF_2.

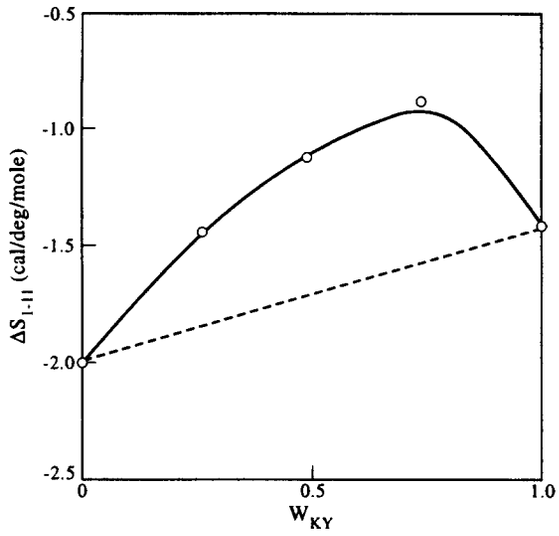

Figure 9 Plot of entropy of activation (ΔS_{I-II}) *versus* blend composition of KF/KY PVF_2 blends

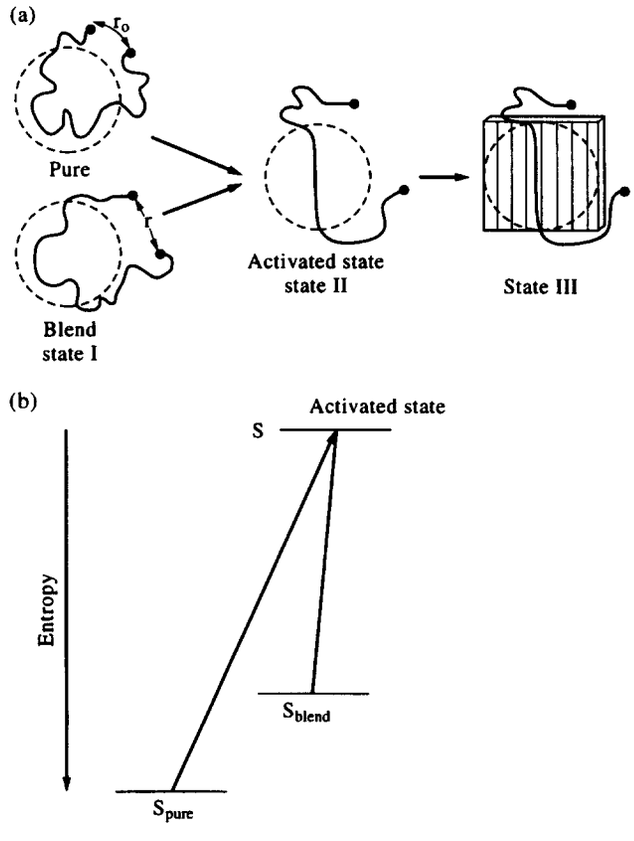

Figure 10 Schematic representation showing loss of entropy to form activated state for crystallisation: (a) from chain configuration; (b) from thermodynamic point of view

Now we want to calculate the entropy of cocrystallisation. Here, it is assumed that the entropy change in the crystallographic attachment of the localised structure (activated state) is the same for both the pure components as well as for the cocrystals. Then the entropy of cocrystallisation can be expressed as:

$$\Delta S_c = \Delta S_{I \to II}^{cocrystal} - \Delta S_{I \to II}^{pure} \quad (7)$$

Using this relation and taking ΔS_{I-II}^{pure} as the arithmetic average of the component values, the ΔS_c values have been calculated and are presented in *Table 5*. From the table it is apparent that $\Delta S_c = \sim 0.6$ cal deg^{-1} mol^{-1}. This is possibly a new approach to calculate the entropy of cocrystallisation during the cocrystal formation from the melt.

CONCLUSION

At the same undercooling the crystallisation rate of the cocrystals is higher than the line joining that of the components. The Avrami exponent varies linearly with composition of cocrystal. Pure KF PVF_2 shows regime I–II transition. KY PVF_2 and the cocrystals exhibit regime II–III transition and it occurs at almost the same undercooling (35 ± 2°C). The $\sigma\sigma_e$ values are lower for the cocrystals than those of the pure components. Analysis of the σ values (with σ_e constant) indicates that in the melt of the blend there is a small extension of the chain and cocrystallisation is an entropy-driven process. The entropy of cocrystallisation has been found to be ~0.6 cal deg^{-1} mol^{-1} for this system.

ACKNOWLEDGEMENTS

We gratefully acknowledge C.S.I.R, New Delhi (grant no.4(112)/91 EMR-11) for financial assistance.

REFERENCES

1. Wang, T. T., Herpart, J. M. and Glass, A. M., in *The Applications of Ferroelectric Polymers*. Blackie & Sons Ltd., London, 1988.
2. Lovinger, A. J., in *Developments in Crystalline Polymers: 1*, ed. D. C. Basset. Applied Science Publishers, London, 1981, p. 195.
3. Farmer, B. L., Hopfinger, A. J. and Lando, J. B., *Journal of Applied Physics*, 1972, **43**, 4293.
4. Lovinger, A. J., Davies, D. D., Cais, R. E. and Kometani, J. M., *Polymer*, 1987, **28**, 617.
5. Datta, J. and Nandi, A. K., *Polymer*, 1994, **35**, 4805.
6. Datta, J. and Nandi, A. K., *Polymer*, 1996, **37**, 5179.
7. Ree, M., Ph. D. Thesis, University of Massachusetts 1987.
8. Iragorri, J. J., Rego, J. M., Katime, I., Conde Braña, M. T. and Gedde, U. W., *Polymer*, 1992, **33**, 461.
9. Tashiro, K., Izuchi, M., Kaneuchi, F., Jin, C., Kobayashi, M. and Stein, R. S., *Macromolecules*, 1994, **27**, 1240.
10. Tashiro, K., Imanishi, K., Izumi, Y., Kobayashi, M., Kobayashi, K., Satoh, M. and Stein, R. S., *Macromolecules*, 1995, **28**, 8477.
11. Hoffman, J. D., Davies, G. T. and Lauritzen, J. I., in *Treatise on Solid State Chemistry*, ed. N. B. Hannay. Plenum Press, New York, 1975, p. 497.
12. Hoffman, J. D., *Polymer*, 1983, **24**, 3.
13. Hoffman, J. D., Miller, R. L., Marand, H. and Roitman, D. B., *Macromolecules*, 1992, **25**, 2221.
14. Marand, H. L., Stein, R. S. and Stack, G. M. J., *Polymer Science, Polymer Physics Edition*, 1988, **26**, 1361.
15. Nakagawa, K. and Ishida, Y. J., *Polymer Science, Polymer Physics Edition*, 1973, **11**, 2153.
16. Morra, B. S. and Stein, R. S., *Journal of Polymer Science, Polymer Physics Edition*, 1982, **20**, 2243.
17. Mandelkern, L., *Crystallization of Polymers*. McGraw-Hill, New York, 1964.
18. Avrami, M., *Journal of Chemical Physics*, 1939, **7**, 1103, ibid, 1940, **8**, 212.
19. Gianotti, G., Cappizzi, A. and Zamboni, V., *Chimica e l'Industria (Milan)*, 1973, **55**, 501.
20. Nakamura, S., Sasaki, T., Funamoto, J. and Matsuzaki, K., *Makromolekulare Chemie*, 1975, **176**, 3471.
21. Mancarella, C. and Martuscelli, E., *Polymer*, 1977, **18**, 1240.
22. Rego Lopez, J. M. and Gedde, U. W., *Polymer*, 1989, **30**, 22.
23. Wood, L. A., *Journal of Polymer Science*, 1958, **28**, 319.
24. Tomura, H., Saito, H. and Inoue, T., *Macromolecules*, 1992, **25**, 1611.
25. Maiti, P. and Nandi, A. K., *Polymer*, in press.

26. Nandi, A. K. and Mandelkern, L., unpublished results.
27. Wang, T. T. and Nishi, T., *Macromolecules*, 1977, **10**, 421.
28. Flory, P. J., *Statistical Mechanics of Chain Molecules*. InterScience Publishers, New York, 1969.
29. Huang, J., Prasad, A., Marand, H. and Roitman, D. B., *Polymer*, 1896, **1994**, 35.
30. Tanaka, H., Lovinger, A. J. and Davies, D. D., *Journal of Polymer Science*, 1990, **B28**, 2183.